An Adaptive Block Backstepping Controller for Attitude Stabilization of a Quadrotor Helicopter

Hongtao Zhen, Xiaohui Qi, Hairui Dong
Unmanned Aerial Vehicle Engineering Department
Mechanical Engineering College
Shijiazhuang, Hebei, 050003
China
oec_ljw2009@sohu.com

Abstract:-A new block backstepping controller is proposed to solve the attitude stabilization problem for a quadrotor helicopter. The attitude kinematical model is obtained and translated into a MIMO nonlinear system with generalized uncertainties. Under the consideration of the coupling between the attitude angles, a nominal block backstepping controller is designed. The obtained controller is then augmented by a robust adaptive function to approximate the modeling errors and external disturbance. A nonlinear tracking-differentiator is applied to reduce computer explosion which is a ubiquitous problem in backstepping controllers. The closed-loop system is proved to be stable and exponential convergent through constructing appropriate Lyapunov function. Simulation results in the presence of external momentary disturbances and parametric uncertainties are presented to corroborate the effectiveness and the robustness of the proposed strategy.

Key-Words: **-** Quadrotor; Block Backstepping; Robust function; Adaptive control; tracking-differentiator

1 Introduction

Quadrotor helicopter is a kind of vertical take-off and landing (VTOL) multi-rotor unmanned aerial vehicles (UAV). In the last few years, the automatic flight control of quadrotor helicopter has been highlighted in a lot of papers [1]-[4]. Nevertheless, this kind of helicopter has a high nonlinear and time-varying behavior and it is constantly affected by aerodynamic disturbances. In addition, helicopters are usually models subject to unmodelled dynamics and parametric uncertainties. Therefore, it is a difficult work to model the system and design related autonomic flight controller. In order to achieve good performance in autonomous flight with high robustness with respect to external disturbances, some advanced nonlinear control methodologies have been applied extensively to the control of quadrotor, such as Feedback linearization [5], [6]and backstepping [7], [8]. Although feedback linearization techniques are widely used in the flight control law design, however, this method relies on a known model of the helicopter with precise parameters. Besides, all of the nonlinear terms are eliminated with this method, which limits its robustness.

Backstepping is a recursive procedure that interlaces the choice of a Lyapunov function with the design of the feedback control. The advantage of this technique is that it can gain from the stabilizing nonlinear terms rather than eliminating them. Backstepping has been applied to a number of different design tasks [9]-[21]. The authors of [10] proposed the backstepping controllers for the rotational control of the quadrotor nonlinear systems. However, this work decoupled the rotational system into three single-input single-output (SISO) subsystems, and didn’t consider the uncertainties. In paper [11], the authors presented an adaptive backstepping controller to estimate and compensate the external disturbances. But also, only the scalar version of backstepping was used and the couple between the three attitude angles was neglected.

In papers [16]-[19] the multi-input multi-output (MIMO) backstepping, also known as block backstepping are investigated and applied. Cao et al. [16] designed an adaptive block backstepping flight controller for a MIMO nonlinear missile system, but this method required the knowledge of the upper bounds of the unknown parameters. Chang [17] proposed a block backstepping controller for the MIMO perturbed systems to achieve asymptotic stability without the knowledge of the upper bounds of perturbations except those of the input uncertainties.

However, the computing expansion problem exists in the backstepping technique. As the order of the system increases, the implementation of backstepping becomes increasingly complex since that the command derivatives are needed to compute at each step of the design. The authors of [20] proposed the dynamic surface control method to solve the computing expansion problem. In this method, a low pass filter was introduced to cancel the repeated differentiations of the demands of the nonlinearities to avoid the complexity caused by expansion of the differential terms. Farrell et al. [21] addressed a modification that obviates the need to compute analytic derivatives by introducing command filters in the backstepping design.

In the paper, an adaptive block backstepping control strategy with robust function is proposed to the problem of controlling the attitude of a quadrotor helicopter described by the full nonlinear 3-degree-of-freedom dynamics. Comparison to the methodologies mentioned above, this work considers the couples between the attitude angles and the uncertainties, and the nonlinear tracking-differentiator developed in [22] is introduced to simplify the algorithm complexity.

The paper is organized as follows. In Section 2 the attitude dynamics of quadrotor are analyzed and the problem is formulated. Then the control architecture is presented in Section 3, including the block backstepping controller, the robust function and the tracking-differentiator. Section 4 represents the stability analysis. The simulation results are presented in Section 5, and then the conclusions are established in Section 6.

2 Quadrotor Dynamics

The main purpose of this paper is to design attitude controller for the quadrotor vehicle, so only the 3-degree-of-freedom attitude model is presented.

2.1 Attitude Kinematics

Given the quadrotor vehicle being a single rigid body, the rotational equations in the fixed body frame which is obtained from the Newton-Euler formalism, can be expressed as (1),

$$\boldsymbol{J}\begin{bmatrix}\dot{p}\\ \dot{q}\\ \dot{r}\end{bmatrix}=\begin{bmatrix}0 & r & -q\\ -r & 0 & p\\ q & -p & 0\end{bmatrix}\boldsymbol{J}\begin{bmatrix}p\\ q\\ r\end{bmatrix}+\begin{bmatrix}L\\ M\\ N\end{bmatrix} \tag{1}$$

where p,q,r represent the angular velocities in the body fixed frame, L,M,N represent the combined external moments in the body fixed frame, $\boldsymbol{J}\in\mathbf{R}^{3\times 3}$ denotes the inertia matrix, the matrix denotes diagonal because of the symmetry of the quadrotor, so $\boldsymbol{J}=\mathrm{diag}(J_x,J_y,J_z)$.

The attitude kinematics equations can be obtained from the rotation relationships between the body fixed frame and the inertial frame as follows,

$$\begin{bmatrix}\dot{\phi}\\ \dot{\theta}\\ \dot{\psi}\end{bmatrix}=\begin{bmatrix}1 & \sin\phi\tan\theta & \cos\phi\tan\theta\\ 0 & \cos\phi & \sin\phi\\ 0 & \sin\phi\sec\theta & \cos\phi\sec\theta\end{bmatrix}\begin{bmatrix}p\\ q\\ r\end{bmatrix} \tag{2}$$

Here ϕ,θ,ψ denote the roll angle, pitch angle and yaw angle respectively.

2.2 Quadrotor Aerodynamics

The modeling of aerodynamic for rotor UAV is very difficult, because the realistic aerodynamic of rotor is very complex both in theory and in formulism. Moreover, the rotors of the mini-quadrotor helicopter are small, light and soft, so it is hard to describe the exact aerodynamics parameters of the rotors. Here, some minute moments act on the quadrotor are reduced, the unmodelled items are considered as external disturbance. It is convenience to design the control law, and it could ensure the reality of the system model at the same time by applying this approach.

The main work of aerodynamics modeling is to analyze the external moments applied on the quadrotor. The moments include

$$\begin{cases} L=L_R+L_G+L_D+L_d\\ M=M_R+M_G+M_D+M_d\\ N=N_R+N_G+N_D+N_d\end{cases} \tag{3}$$

where the subscript R,G,D,d represent the thrust moments, gyroscopic effects, drag moments and external disturbance moments, respectively.

The moments produced by rotor thrust are

$$\boldsymbol{M}_R=\begin{bmatrix}L_R\\ M_R\\ N_R\end{bmatrix}=\begin{bmatrix}lk_L(\omega_2^2-\omega_4^2)\\ lk_L\left(\omega_3^2-\omega_1^2\right)\\ k_Q\left(\omega_1^2-\omega_2^2+\omega_3^2-\omega_4^2\right)\end{bmatrix} \tag{4}$$

where k_L represent the lift coefficient which is related to the rotor area, rotor radius and air density, ω_i represent the rotor rotate speed, l represent the vertical distance from motor shaft to the center of mass of the quadrotor, k_Q represent the reaction torque coefficient.

The gyroscopic effect is the additional torque, which is produced by the rotating rotors with high speed, when the quadrotor works, it can avoid pitch or roll. The gyroscopic effects can be written as follows,

$$\boldsymbol{M}_G = \begin{bmatrix} L_G \\ M_G \\ N_G \end{bmatrix} = \begin{bmatrix} j_r q\bar{\varpi} \\ -j_r p\bar{\varpi} \\ 0 \end{bmatrix} \tag{5}$$

where j_r represents the rotational inertia of rotors, and $\bar{\varpi} = (-\omega_1 + \omega_2 - \omega_3 + \omega_4)$.

The drag moments are expressed as,

$$\boldsymbol{M}_D = \begin{bmatrix} L_D \\ M_D \\ N_D \end{bmatrix} = \begin{bmatrix} k_{Dx} p \\ k_{Dy} q \\ k_{Dz} r \end{bmatrix} \tag{6}$$

where k_{Dx}, k_{Dy} and k_{Dz} are the triaxial air drag coefficients in the body fixed frame.

As the area and rotational inertial of quadrotor researched in the paper are small, and the angular velocities are slow, so the gyroscopic effects and drag moments can be ignored. And then the external moments can be expressed as

$$\begin{cases} L = L_R + \Delta_L + L_d \\ M = M_R + \Delta_M + M_d \\ N = N_R + \Delta_N + N_d \end{cases} \tag{7}$$

where $\Delta_L = L_G + L_D$, $\Delta_M = M_G + M_D$, $\Delta_N = N_G + N_D$ denote the unmodelled terms which are ignored. From the expression above, the attitude kinematic equations can be written as (8),

$$\begin{cases} \dot{\phi} = p + (q\sin\phi + r\cos\phi)\tan\theta \\ \dot{\theta} = q\cos\phi - r\sin\phi \\ \dot{\psi} = (q\sin\phi + r\cos\phi)\sec\theta \\ \dot{p} = a_1 qr + b_1 k_L(\omega_2^2 - \omega_4^2) + \Delta_1 \\ \dot{q} = a_2 pr + b_2 k_L(\omega_3^2 - \omega_1^2) + \Delta_2 \\ \dot{r} = a_3 qr + b_3 k_Q(\omega_1^2 - \omega_2^2 + \omega_3^2 - \omega_4^2) + \Delta_3 \end{cases} \tag{8}$$

where

$$\begin{cases} a_1 = \dfrac{J_y - J_z}{J_x} \\ a_2 = \dfrac{J_z - J_x}{J_y} \\ a_3 = \dfrac{J_x - J_y}{J_z} \end{cases} \tag{9}$$

$$\begin{cases} b_1 = \dfrac{l}{J_x} \\ b_2 = \dfrac{l}{J_y} \\ b_3 = \dfrac{1}{J_z} \end{cases} \tag{10}$$

$$\begin{cases} \Delta_1 = \dfrac{\Delta_L + L_d}{J_x} \\ \Delta_2 = \dfrac{\Delta_M + M_d}{J_y} \\ \Delta_3 = \dfrac{\Delta_N + N_d}{J_z} \end{cases} \tag{11}$$

2.3 State-space Modeling

If we set the parameters as below,

$$\boldsymbol{x}_1 = \begin{bmatrix} \phi \\ \theta \\ \psi \end{bmatrix} \tag{12}$$

$$\boldsymbol{x}_2 = \begin{bmatrix} p \\ q \\ r \end{bmatrix} \tag{13}$$

$$\boldsymbol{u} = \begin{bmatrix} k_L(\omega_2^2 - \omega_4^2) \\ k_L\left(\omega_3^2 - \omega_1^2\right) \\ k_Q\left(\omega_1^2 - \omega_2^2 + \omega_3^2 - \omega_4^2\right) \end{bmatrix} \tag{14}$$

then, in general form of MIMO nonlinear system state-space model, the equation (8) can be rewritten as follows,

$$\begin{aligned} \dot{\boldsymbol{x}}_1 &= \boldsymbol{f}_1(\boldsymbol{x}_1) + \boldsymbol{b}_1(\boldsymbol{x}_1)\boldsymbol{x}_2 \\ \dot{\boldsymbol{x}}_2 &= \boldsymbol{f}_2(\boldsymbol{x}_1, \boldsymbol{x}_2) + \boldsymbol{b}_2(\boldsymbol{x}_1, \boldsymbol{x}_2)\boldsymbol{u} \end{aligned} \tag{15}$$

where

$$\boldsymbol{f}_1 = \boldsymbol{0}_{3\times 3} \tag{16}$$

$$\boldsymbol{b}_1 = \begin{bmatrix} 1 & \sin\phi\tan\theta & \cos\phi\tan\theta \\ 0 & \cos\phi & \sin\phi \\ 0 & \sin\phi\sec\theta & \cos\phi\sec\theta \end{bmatrix} \tag{17}$$

$$\boldsymbol{f}_2 = \boldsymbol{f}_{20} + \Delta\boldsymbol{f}_2 = \begin{bmatrix} a_1 qr \\ a_2 pr \\ a_3 pq \end{bmatrix} + \begin{bmatrix} \Delta_1 \\ \Delta_2 \\ \Delta_3 \end{bmatrix} \tag{18}$$

$$\boldsymbol{b}_2 = \boldsymbol{b}_{20} + \Delta\boldsymbol{b}_2 = \begin{bmatrix} b_1 & 0 & 0 \\ 0 & b_2 & 0 \\ 0 & 0 & b_3 \end{bmatrix} + \begin{bmatrix} \Delta b_1 & 0 & 0 \\ 0 & \Delta b_1 & 0 \\ 0 & 0 & \Delta b_1 \end{bmatrix} \quad (19)$$

here $\boldsymbol{f}_{20}$ and $\boldsymbol{b}_{20}$ represent the nominal system, $\Delta\boldsymbol{f}_2$ denotes the unmodelled terms and external disturbance, $\Delta\boldsymbol{b}_2$ denotes the system parametric perturbations.

3 Attitude Controller Design

3.1 Block Backstepping Control

In order to obtain precise result, we introduce the new two three-dimensional error state vectors $\tilde{\boldsymbol{x}}_1, \tilde{\boldsymbol{x}}_2$ in the analysis, which can be expressed as below,

$$\begin{aligned} \tilde{\boldsymbol{x}}_1 &= \boldsymbol{x}_1 - \boldsymbol{x}_{1d} \\ \tilde{\boldsymbol{x}}_2 &= \boldsymbol{x}_2 - \boldsymbol{x}_{2d} \end{aligned} \quad (20)$$

where $\boldsymbol{x}_{1d}$ and $\boldsymbol{x}_{2d}$ are the reference state vectors, if we substitute the expression (20) into the state-space equation (15), the error dynamic equations can be obtained.

$$\dot{\tilde{\boldsymbol{x}}}_1 = \boldsymbol{f}_1 + \boldsymbol{b}_1\boldsymbol{x}_2 - \dot{\boldsymbol{x}}_{1d} \quad (21)$$

$$\dot{\tilde{\boldsymbol{x}}}_2 = \boldsymbol{f}_2 + \boldsymbol{b}_2\boldsymbol{u} - \dot{\boldsymbol{x}}_{2d} \quad (22)$$

When the error equations are obtained, the design of block backstepping controller can be divided into two steps.

Step 1

According to the error subsystem equation (21), the expected virtual control law $\boldsymbol{x}_{2d}$ is defined as

$$\boldsymbol{x}_{2d} = -\boldsymbol{b}_1^{-1}(\boldsymbol{f}_1 - \dot{\boldsymbol{x}}_{1d} + k_1\tilde{\boldsymbol{x}}_1) \quad (23)$$

where $k_1 > 0$ represents the designed constant. In subsystem (21), we apply the following Lyapunov function,

$$V_1 = \frac{1}{2}\tilde{\boldsymbol{x}}_1^{\mathrm{T}}\tilde{\boldsymbol{x}}_1 \quad (24)$$

if we take the virtual control variable $\boldsymbol{x}_{2d}$ equation (23) into account, the time derivative of the Lyapunov function can be determined by

$$\begin{aligned} \dot{V}_1 &= \tilde{\boldsymbol{x}}_1^{\mathrm{T}}\dot{\tilde{\boldsymbol{x}}}_1 = \tilde{\boldsymbol{x}}_1^{\mathrm{T}}(\boldsymbol{f}_1 + \boldsymbol{b}_1\boldsymbol{x}_2 - \dot{\boldsymbol{x}}_{1d}) \\ &= \tilde{\boldsymbol{x}}_1^{\mathrm{T}}\left[\boldsymbol{f}_1 - \boldsymbol{b}_1\boldsymbol{b}_1^{-1}(\boldsymbol{f}_1 - \dot{\boldsymbol{x}}_{1d} + k_1\tilde{\boldsymbol{x}}_1) - \dot{\boldsymbol{x}}_{1d}\right] \\ &= -k_1\tilde{\boldsymbol{x}}_1^{\mathrm{T}}\tilde{\boldsymbol{x}}_1 = -k_1\left\|\tilde{\boldsymbol{x}}_1\right\|^2 \end{aligned} \quad (25)$$

Hence, from the Lyapunov stability theory, we can find that the subsystem (21) is Lyapunov stable under the condition $\tilde{\boldsymbol{x}}_2 = 0$.

Step 2

The error subsystem equation (22) also can be rewritten as

$$\begin{aligned} \dot{\tilde{\boldsymbol{x}}}_2 &= \boldsymbol{f}_{20} + \boldsymbol{b}_{20}\boldsymbol{u} - \dot{\boldsymbol{x}}_{2d} + \Delta\boldsymbol{f}_2 + \Delta\boldsymbol{b}_2\boldsymbol{u} \\ &= \boldsymbol{f}_{20} + \boldsymbol{b}_{20}\boldsymbol{u} - \dot{\boldsymbol{x}}_{2d} + \boldsymbol{\varDelta} \end{aligned} \quad (26)$$

where $\boldsymbol{\varDelta} = \Delta\boldsymbol{f}_2 + \Delta\boldsymbol{b}_2\boldsymbol{u}$ is the additional uncertain term for the generalized uncertainties.

In the subsystem (22), the ideal control law can be expressed as

$$\boldsymbol{u}^* = -\boldsymbol{b}_{20}^{-1}\left[k_2\tilde{\boldsymbol{x}}_2 + \boldsymbol{f}_{20} + \boldsymbol{b}_1^{\mathrm{T}}\tilde{\boldsymbol{x}}_1 - \dot{\boldsymbol{x}}_{2d} + \boldsymbol{\varDelta}\right] \quad (27)$$

where $k_2 > 0$ is a designed constant. In the Lyapunov function

$$V_2 = \frac{1}{2}\tilde{\boldsymbol{x}}_1^{\mathrm{T}}\tilde{\boldsymbol{x}}_1 + \frac{1}{2}\tilde{\boldsymbol{x}}_1^{\mathrm{T}}\tilde{\boldsymbol{x}}_2 \quad (28)$$

if we take the ideal control law (27) into account, the time derivative of Lyapunov function can be expressed as

$$\begin{aligned} \dot{V}_2 &= \tilde{\boldsymbol{x}}_1^{\mathrm{T}}\left[\boldsymbol{f}_1 + \boldsymbol{b}_1\left(\boldsymbol{x}_{2d} + \tilde{\boldsymbol{x}}_2\right) - \dot{\boldsymbol{x}}_{1d}\right] + \tilde{\boldsymbol{x}}_2^{\mathrm{T}}\left(\boldsymbol{f}_2 + \boldsymbol{b}_2\boldsymbol{u}^* - \dot{\boldsymbol{x}}_{2d}\right) \\ &= \tilde{\boldsymbol{x}}_1^{\mathrm{T}}\left[\boldsymbol{b}_1\tilde{\boldsymbol{x}}_2 - k_1\tilde{\boldsymbol{x}}_1\right] + \tilde{\boldsymbol{x}}_2^{\mathrm{T}}\left(\boldsymbol{f}_2 + \boldsymbol{b}_2\boldsymbol{u}^* - \dot{\boldsymbol{x}}_{2d}\right) \\ &= -k_1\tilde{\boldsymbol{x}}_1^{\mathrm{T}}\tilde{\boldsymbol{x}}_1 + \tilde{\boldsymbol{x}}_1^{\mathrm{T}}\boldsymbol{b}_1\tilde{\boldsymbol{x}}_2 - k_2\tilde{\boldsymbol{x}}_2^{\mathrm{T}}\tilde{\boldsymbol{x}}_2 - \tilde{\boldsymbol{x}}_2^{\mathrm{T}}\boldsymbol{b}_1^{\mathrm{T}}\tilde{\boldsymbol{x}}_1 \\ &= -k_1\left\|\tilde{\boldsymbol{x}}_1\right\|^2 - k_2\left\|\tilde{\boldsymbol{x}}_2\right\|^2 \end{aligned} \quad (29)$$

Therefore, the whole system (15) will be Lyapunov stable if the control law is satisfied with equation (27).

3.2 Robust Function

From the equation (27), it can be found that there is an unknown uncertain term $\boldsymbol{\varDelta}$ in the ideal control law, so the control law is unrealistic. In this section, a robust function is proposed in order to avoid the effect of uncertainties.

If uncertainties of the system are bounded and they are also governed by a nonnegative smooth function which is with an unknown constant. We can make the assumption as that there exists an unknown positive constant ρ, there also exists the relationship as (29),

$$\left\|\boldsymbol{\varDelta}\right\| \le \rho\delta(\boldsymbol{x}_1, \boldsymbol{x}_2) \quad (29)$$

where $\delta(\boldsymbol{x}_1, \boldsymbol{x}_2)$ is a known nonnegative smooth function.

The robust function $\boldsymbol{\eta}$ is expressed as

$$\boldsymbol{\eta} = \tilde{\boldsymbol{x}}_2\hat{\rho}^2\delta^2 \quad (30)$$

where $\hat{\rho}$ is the estimated value of the unknown constant ρ. The following adaptive law is proposed according to the unknown parameter,

$$\dot{\hat{\rho}} = \gamma \left\| \tilde{\boldsymbol{x}}_2 \right\| \delta - k_3 \hat{\rho} \tag{31}$$

where γ and k_3 represent the positive designed parameters, respectively, the sign $\|\cdot\|$ denotes 2-norm.

When introducing and analyzing of the robust function are finished, the ideal control law (27) can be rewritten as

$$\boldsymbol{u} = -\boldsymbol{b}_{20}^{-1}\left[k_2 \tilde{\boldsymbol{x}}_2 + \boldsymbol{f}_{20} + \boldsymbol{b}_1^{\mathrm{T}} \tilde{\boldsymbol{x}}_1 - \dot{\boldsymbol{x}}_{2d} + \boldsymbol{\eta} \right] \tag{32}$$

3.3 Nonlinear Tracking-differentiator

Control law equation (32) includes the differential item $\dot{\boldsymbol{x}}_{2d}$, from the equilibrium (23) we know that $\boldsymbol{x}_{2d}$ is a function related to $\boldsymbol{f}_1$, $\boldsymbol{b}_1$, $\boldsymbol{x}_1$, $\boldsymbol{x}_{1d}$, $\dot{\boldsymbol{x}}_{1d}$, the time derivative of $\boldsymbol{x}_{2d}$ is given by

$$\dot{\boldsymbol{x}}_{2d} = \frac{\delta \boldsymbol{x}_{2d}}{\delta \boldsymbol{f}_1} \dot{\boldsymbol{f}}_1 + \frac{\delta \boldsymbol{x}_{2d}}{\delta \boldsymbol{b}_1} \dot{\boldsymbol{b}}_1 + \frac{\delta \boldsymbol{x}_{2d}}{\delta \boldsymbol{x}_1} \dot{\boldsymbol{x}}_1 + \frac{\delta \boldsymbol{x}_{2d}}{\delta \boldsymbol{x}_{1d}} \dot{\boldsymbol{x}}_{1d} + \frac{\delta \boldsymbol{x}_{2d}}{\delta \dot{\boldsymbol{x}}_{1d}} \ddot{\boldsymbol{x}}_{1d} \tag{33}$$

Hence, the calculation of $\dot{\boldsymbol{x}}_{2d}$ is very complicated, it will lead to computing expansion if we differentiate $\boldsymbol{x}_{2d}$ directly. In order to avoid this problem, the nonlinear tracking-differentiator is proposed and applied to calculate the estimated value of $\dot{\boldsymbol{x}}_{2d}$.

The second-order fastest tracking-differentiator developed in [22] is adopted in this paper. This differentiator can avoid the noise amplification effect of traditional linear differentiator, and it can trace the input signal very fast. It can be expressed as below

$$\begin{cases} \dot{z}_1 = z_2 \\ \dot{z}_2 = -r \operatorname{sign}\left(z_1 - v(t) + \dfrac{z_2 |z_2|}{2r} \right) \end{cases} \tag{34}$$

where r is a positive designed parameters, $v(t)$ is the input signal, the sign$(\cdot)$ represents sign function.

In the design, $\boldsymbol{x}_{2d}$ is the input signal of the tracking-differentiator, the output signal part z_1 is $\hat{\boldsymbol{x}}_{2d}$, which is the estimated value of $\boldsymbol{x}_{2d}$. The state variable z_2 is the approximate value of $\dot{\boldsymbol{x}}_{2d}$.

Finally, the practical feedback control law can be given by

$$\boldsymbol{u} = -\boldsymbol{b}_{20}^{-1}\left[k_2 \tilde{\boldsymbol{x}}_2 + \boldsymbol{f}_{20} + \boldsymbol{b}_1^{\mathrm{T}} \tilde{\boldsymbol{x}}_1 - \dot{\hat{\boldsymbol{x}}}_{2d} + \boldsymbol{\eta} \right] \tag{35}$$

4 Stability Analysis

The parametric estimation error can be defined as

$$\tilde{\rho} = \hat{\rho} - \rho \tag{36}$$

For whole closed-loop system, define the candidate Lyapunov function

$$V = \frac{1}{2} \tilde{\boldsymbol{x}}_1^{\mathrm{T}} \tilde{\boldsymbol{x}}_1 + \frac{1}{2} \tilde{\boldsymbol{x}}_2^{\mathrm{T}} \tilde{\boldsymbol{x}}_2 + \frac{1}{2\gamma} \tilde{\rho}^2 \tag{37}$$

the time derivative of V takes the form:

$$\begin{aligned} \dot{V} &= \tilde{\boldsymbol{x}}_1^{\mathrm{T}} \dot{\tilde{\boldsymbol{x}}}_1 + \tilde{\boldsymbol{x}}_2^{\mathrm{T}} \dot{\tilde{\boldsymbol{x}}}_2 + \frac{1}{\gamma} \tilde{\rho} \dot{\tilde{\rho}} \\ &= -k_1 \tilde{\boldsymbol{x}}_1^{\mathrm{T}} \tilde{\boldsymbol{x}}_1 + \tilde{\boldsymbol{x}}_1^{\mathrm{T}} \boldsymbol{b}_1 \tilde{\boldsymbol{x}}_2 - k_2 \tilde{\boldsymbol{x}}_2^{\mathrm{T}} \tilde{\boldsymbol{x}}_2 - \tilde{\boldsymbol{x}}_2^{\mathrm{T}} \boldsymbol{b}_1^{\mathrm{T}} \tilde{\boldsymbol{x}}_1 \\ &\quad + \tilde{\boldsymbol{x}}_2^{\mathrm{T}} \left(\boldsymbol{\Delta} - \boldsymbol{\eta} \right) + \frac{1}{\gamma} \tilde{\rho} \dot{\tilde{\rho}} \\ &\le -k_1 \tilde{\boldsymbol{x}}_1^{\mathrm{T}} \tilde{\boldsymbol{x}}_1 - k_2 \tilde{\boldsymbol{x}}_2^{\mathrm{T}} \tilde{\boldsymbol{x}}_2 + \rho \left\| \tilde{\boldsymbol{x}}_2 \right\| \delta - \left\| \tilde{\boldsymbol{x}}_2 \right\|^2 \hat{\rho}^2 \delta^2 \\ &\quad + \frac{1}{\gamma} \tilde{\rho} \left(\gamma \left\| \tilde{\boldsymbol{x}}_2 \right\| \delta - k_3 \hat{\rho} \right) \end{aligned} \tag{38}$$

If we put equation (36) and the identical equation $-\tilde{\rho}\hat{\rho} = -\frac{1}{2}\tilde{\rho}^2 - \frac{1}{2}\hat{\rho}^2 + \frac{1}{2}\rho^2$ into equation (38), the following expression is obtained,

$$\begin{aligned} \dot{V} &\le -k_1 \tilde{\boldsymbol{x}}_1^{\mathrm{T}} \tilde{\boldsymbol{x}}_1 - k_2 \tilde{\boldsymbol{x}}_2^{\mathrm{T}} \tilde{\boldsymbol{x}}_2 + \hat{\rho} \left\| \tilde{\boldsymbol{x}}_2 \right\| \delta - \hat{\rho}^2 \left\| \tilde{\boldsymbol{x}}_2 \right\|^2 \delta^2 - \frac{k_3}{\gamma} \tilde{\rho} \hat{\rho} \\ &= -k_1 \tilde{\boldsymbol{x}}_1^{\mathrm{T}} \tilde{\boldsymbol{x}}_1 - k_2 \tilde{\boldsymbol{x}}_2^{\mathrm{T}} \tilde{\boldsymbol{x}}_2 - \left(\hat{\rho} \left\| \tilde{\boldsymbol{x}}_2 \right\| \delta - \frac{1}{2} \right)^2 + \frac{1}{4} - \frac{1}{2} \frac{k_3}{\gamma} \tilde{\rho}^2 \\ &\quad - \frac{1}{2} \frac{k_3}{\gamma} \hat{\rho}^2 + \frac{1}{2} \frac{k_3}{\gamma} \rho^2 \\ &\le -k_1 \tilde{\boldsymbol{x}}_1^{\mathrm{T}} \tilde{\boldsymbol{x}}_1 - k_2 \tilde{\boldsymbol{x}}_2^{\mathrm{T}} \tilde{\boldsymbol{x}}_2 - \frac{1}{2} \frac{k_3}{\gamma} \tilde{\rho}^2 + \frac{1}{4} + \frac{1}{2} \frac{k_3}{\gamma} \rho^2 \\ &\le -c_0 V + c_1 \end{aligned} \tag{39}$$

where

$$c_0 = \min\left\{ k_1, k_2, \frac{k_3}{2\gamma} \right\}, \quad c_1 = \frac{1}{4} + \frac{k_3}{2\gamma} \rho^2 .$$

When we finish the solving of inequation $\dot{V} \le -c_0 V + c_1$, the equation (40) will be obtained,

$$\begin{aligned} V(t) &\le V(0) \exp(-c_0 t) + \frac{c_1}{c_0} \left[1 - \exp(-c_0 t) \right] \\ &\le V(0) + \frac{c_1}{c_0} \qquad \forall t \ge 0 \end{aligned} \tag{40}$$

where $V(0)$ represent the initial value of $V(t)$.The solution of (40) implies that the Lyapunov function $V(t)$ is bounded, i.e., all the signals in the close loop system are bounded. If we adjust the designed parameter to satisfy with the conditions $c_0 > 0$ and $c_0 \ge c_1 / V(0)$, and it will leads to $\dot{V} < 0$. Thus, it can prove the system is Lyapunov stable and the errors are asymptotically converge to an arbitrarily small neighborhood of zero,

$$\{\tilde{x}_1, \tilde{x}_2, \tilde{\rho}\} \in \boldsymbol{\Omega} = \left\{ \boldsymbol{X} \mid V(\boldsymbol{X}) \le V(0) + \frac{c_1}{c_0} \right\} \quad (41)$$

The converging speed and the domain of convergence are determined by the designed parameters k_1, k_2, k_3, γ .

5 Simulation Results

In order to check and analyze the performances, the proposed control strategy is tested by simulations in the software of MATLAB. Besides, simulations comparing the control structure proposed above with the traditional backstepping approach are also performed.

If we set the initial states of the quadrotor with $\boldsymbol{x}_1 = [0.5, 0.5, 0.5]^{\mathrm{T}}$, the nonnegative smooth function is $\delta = |\sin\|\boldsymbol{x}_2\|| + |\cos\|\boldsymbol{x}_2\||$. The control purpose is to stabilitate the helicopter at the origin in the fixed inertial frame, that is, $\boldsymbol{x}_d = [0,0,0]^{\mathrm{T}}$ and $\dot{\boldsymbol{x}}_{1d} = 0$. The sampling period is 2ms, the values of the model parameters and controller parameters in the simulations are presented in Table 1.

Table 1 Parameters of the simulation model

Model Parameters		Controller Parameters	
l / m	0.230	k_1	1
$J_x / (\mathrm{kg \cdot m^2})$	0.008	k_2	8
$J_y / (\mathrm{kg \cdot m^2})$	0.008	k_3	2
$J_z / (\mathrm{kg \cdot m^2})$	0.013	γ	10

In order to verify the robustness of the proposed approach, the various uncertainties of quadrotor may be subjected in flight are considered, four simulation experiments are performed in the paper.

5.1 Constant Moment Disturbance

If we make the assumption that the quadrotor is subjected to persistent constant moment disturbances expressed as formula (42), the disturbances are added to the control inputs at 5, 10, 15 seconds in the roll, pitch and yaw channel, respectively. The results obtained are shown in Fig.1and Fig.2.

In Fig.1, it can be seen that, the two controllers both can control the quadrotor from the initial state to stable state. However, the convergence speed of the adaptive block backstepping control is little slower than the nominal backstepping control. Under the disturbance of constant moment, the steady state error of the attitude angle in the nominal backstepping control is about 0.09rad, while the steady state error in the adaptive block backstepping control with robust function is less than 0.006rad. These results indicate that the proposed control structure is more robust than the nominal block backstepping control under the condition of constant moment disturbance.

From Fig.2 we can see that the fluctuations of angular velocities of adaptive backstepping are also smaller than the nominal backstepping.

$$\boldsymbol{\Delta} = \begin{cases} [0,0,0]^{\mathrm{T}} & t < 5\mathrm{s} \\ [1,0,0]^{\mathrm{T}} & 5 \le t < 10\mathrm{s} \\ [1,1,0]^{\mathrm{T}} & 10 \le t < 15\mathrm{s} \\ [1,1,1]^{\mathrm{T}} & t \ge 15\mathrm{s} \end{cases} \quad (42)$$

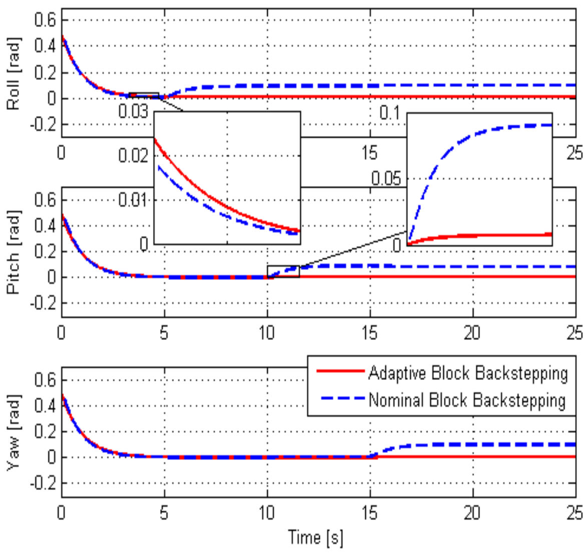

Fig.1 Output angles with constant moment disturbance

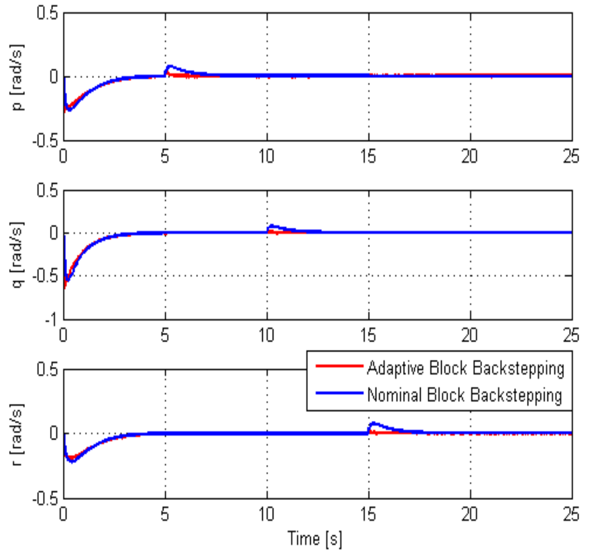

Fig.2 Angular velocities with constant moment disturbance

5.2 Transient Moment Disturbance

In order to test the robustness of the quadrotor to wind gusts disturbance, the transient moment disturbances are added to the simulation model. The simulation results are shown in Fig.3 and Fig.4, the transient moment disturbances are given by

$$\Delta = \begin{cases} [0,0,0]^{\mathrm{T}} & t < 10\mathrm{s} \\ [1,1,1]^{\mathrm{T}} & 10 \le t < 12\mathrm{s} \\ [0,0,0]^{\mathrm{T}} & t \ge 12\mathrm{s} \end{cases} \tag{43}$$

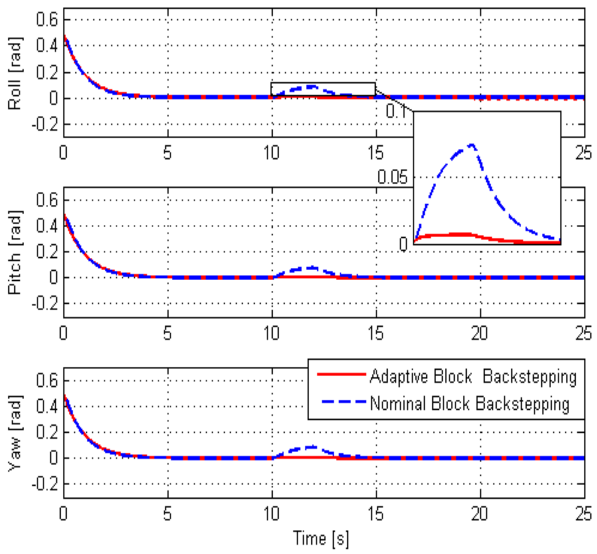

Fig.3 Output angles with transient moment disturbance

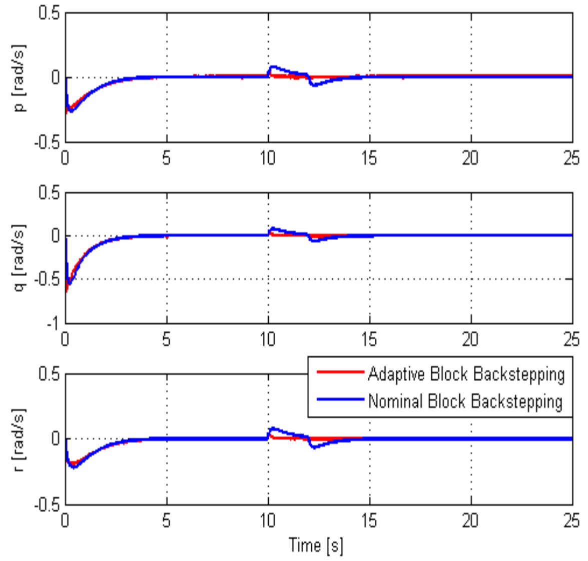

Fig.4 Angular velocities with transient moment disturbance

In Fig.3, we can find that the output angles perturb when the disturbances occur, it also can be seen from the partial enlarged details that the instantaneous error of the roll angle with the nominal backstepping control is about 0.09rad, while the error with the adaptive backstepping control is only 0.007rad. These results demonstrate that the robustness of proposed control strategy is improved apparently compare to the nominal backstepping control with the transient moment disturbance when the quadrotor is stable.

It is obvious that the angular velocities under nominal block backstepping control change obviously when the disturbances coming which is shown as Fig. 4. But the angular velocities under adaptive block backstepping control are not changed almost.

5.3 Sine Moment Disturbance

It is inevitably to encounter the persistent gusts of wind sometime when the helicopter flies in the sky, in order to make further investigations on the performance of the proposed control, the sine moment disturbances are added to the system for simulation of effects of the persistent gusts. Simulation results are given out in Fig.5 and Fig.6, the mathematic equation of the sine moment disturbances can be written as (44),

$$\Delta = \sin(t)[1,1,1]^{\mathrm{T}} \tag{44}$$

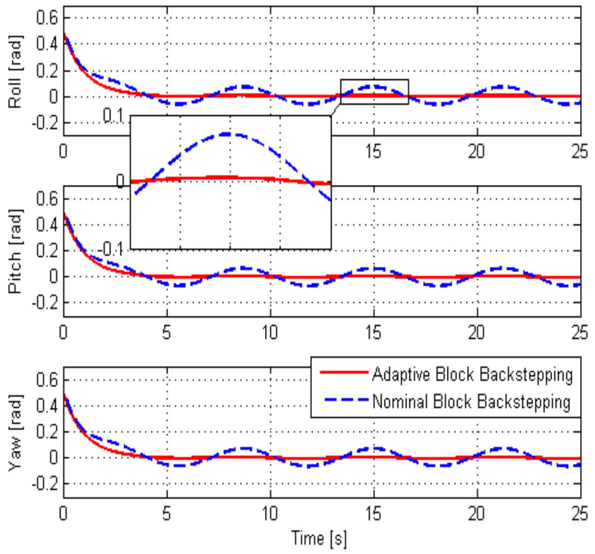

Fig.5 Output angles with sine moment disturbance

It can be observed from Fig.5 that the maximum roll angle error is about 0.07rad applying the nominal backstepping control. Although there are some errors in the robust adaptive block backstepping control, while the maximum error is only 0.005rad. Moreover, the convergence speed is faster than the nominal traditional control. It is obvious that the proposed adaptive backstepping control structure is also robust when it is added low-frequency sine disturbance moments.

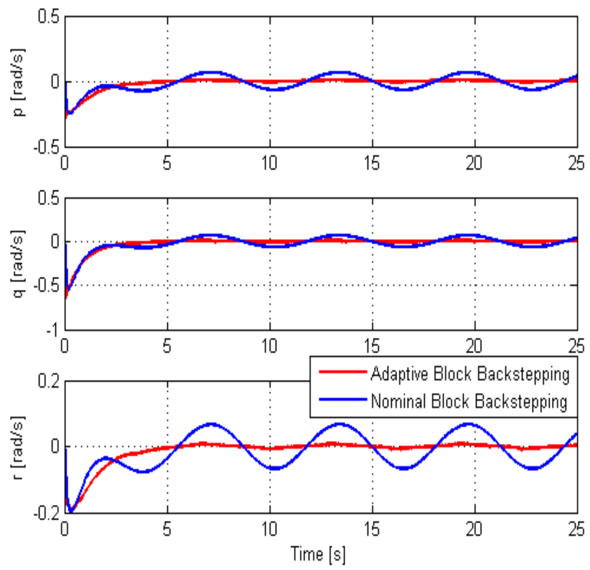

Fig.6 Angular velocities with sine moment disturbance

And the convergence speed is faster than the nominal control. Moreover, the fluctuations of angular velocities are smaller than that using nominal block backstepping which illustrated as in Fig.6.

5.4 System Parametric Perturbation

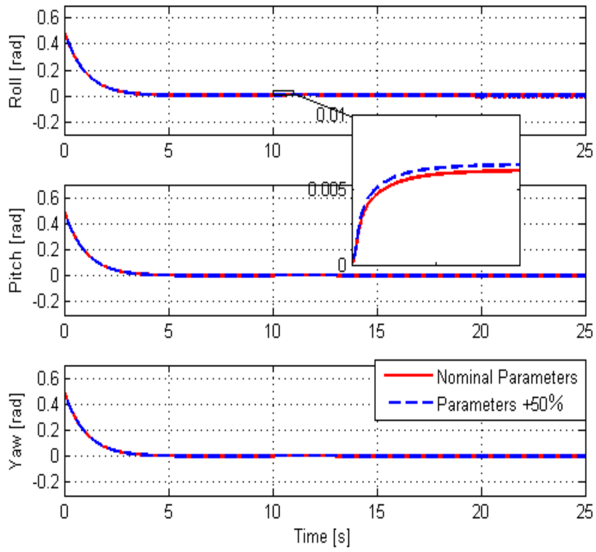

Fig.7 Output angles with parameters perturb +50%

Some parameters in the system may be inaccurate and some parameters also may change with time. In order to test the robustness of control with parameter perturbation, the +30% uncertainty of the system matrix $\boldsymbol{b}$ and the transient moment disturbance in (43) are considered in the simulation, the simulation results obtained are shown in Fig.7 and Fig.8.

In Fig.7, the output angles are quite similar to the case that with standard parameters of system, the instantaneous error enlarges 6.67% only when the transient disturbance exists. The results indicate that the proposed controller still presents robust to parametric perturbation.

From the partial enlarged details of Fig. 8, we can find that the angular velocities of the two controllers are almost same.

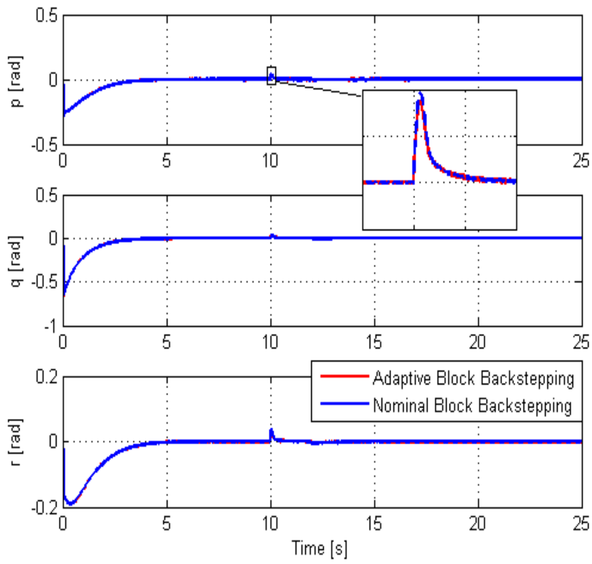

Fig.8 Angular velocities with parameters perturb +50%

6. Conclusions

An adaptive block backstepping control strategy is proposed to solve the attitude stabilization problem of the quadrotor helicopter in the paper. Firstly, the full nonlinear three-degree-of-freedom attitude dynamics are described under consideration of internal uncertainties and external disturbances acting on all degrees of freedom. Then, the block backstepping controller with a robust adaptive function is proposed. Against the computing expansion problem, a second order nonlinear tracking-differentiator is applied into the controller. The stability of the close loop system is ensured according to the Lyapunov stable theory. Finally, the numerical simulation results illustrate the robustness and smoothness of the provided controller in the case of constant moment disturbance, transient moment disturbance, sine moment disturbance and system parametric Perturbation.

As a future work we will implement this control strategy in a real quadrotor helicopter. A new vehicle is being built, which will include appropriate control hardware to compute control signals.

Acknowledgements

The Authors would like to thank Dr. J.W.LV for critically evaluating the manuscript and the control group members of UAV staff room for their kind help at various stages of the research.

This project is supported by the National Defense Research Fund of China. This is also partially supported by the Science Fund of China.

References

[1] Guiherme V, Manuel G, Francisco R. An integral predictive/nonlinear H_∞ control structure for a quadrotor helicopter. *Automatica*, 2010 (46): 29-39.

[2] David L, Gerardo R, Anand S, et al. Robustness margin for attitude control of a four rotor mini-rotorcraft: case of study. *Mechatronics*, 2010(20): 143-152.

[3] Samir B, Pierpaolo M, Roland S. Toward autonomous indoor micro VTOL. *Autonomous Robots*, 2005(18): 171-183.

[4] Toledo J, Acosta L, Sigut M, et al. Stabilisation and altitude tracking of a four-rotor microhelicopter using the lifting operators. *IET Control Theory Application*, 2009(3): 452-464.

[5] Kanellakopoulos I, Kokotovic V, Morse S. Systematic Design of Adaptive Controller for Feedback Linearizable System. *IEEE Transactions on Automatic Control*, 1991, 36(11): 1241-1253.

[6] Zhou Fang, Zhang Zhi, Liang Jun, et al. Feedback linearization and continuous sliding mode control for a quadrotor UAV. *Proceedings of the 27th Chinese Control Conference*, 2008: 349-353.

[7] Tarek M, Abdelaziz B. Backstepping control for a quadrotor helicopter. *International Conference on Intelligent Robots and Systems*, 2006: 3255-3259.

[8] Guiherme V, Manuel G, Francisco R. Backstepping/H_∞ control for path tracking of a quadrotor unmanned aerial vehicle. *Proceeding of the American Control Conference*, 2008: 3356-3361.

[9] Belkheiri M, Boudjema F. Function approximation based augmented backstepping control for an induction machine. *WSEAS Transactions on Systems and Control*, (2), pp.450-457, 2007.

[10] Ashfaq A M, Wang Daobo. Modeling and backstepping-based nonlinear control strategy for a 6 DOF quadrotor helicopter. *Chinese Journal of Aeronautics*, (21), pp.261-268, 2008.

[11] Liu H Y, Li J, Yao J G, et al. Backstepping based adaptive control for a mini rotorcraft with four rotors. *The Second International Conference on Computer Modeling and Simulation*, 2010: 472-476.

[12] Madani T, Benallegue A. Sliding mode observer and backstepping control for a quadrotor unmanned aerial vehicles. *Proceedings of the American Control Conference*, 2007: 5887-5892.

[13] Guenard N, Hamel T, Mahony R. A practical visual servo control for an unmanned aerial vehicle. *Robotics*, 2008, 24(2): 331-340.

[14] Lee T, Kim Y. Nonlinear adaptive flight control using backstepping and neural networks controller. *Journal of Dynamic Systems, Measurement and Control*, 2005, 127(3): 478-485.

[15] Ren W, Atkins E. Nonlinear trajectory tracking for fixed wing UAVs via backstepping and parameter adaptation. *AIAA Guidance, Navigation and Control Conference and Exhibit*, 2005.

[16] Cao L J, Zhang S X, Liu Y N, et al. Flight controller design using adaptive parameter approximation block backstepping. *Acta*

Aeronautica et Astronautica Sinica, 2011, 32(12): 2259-2267.

[17] Chang Yaote. Block backstepping control of MIMO systems. *IEEE Transactions on Automatic Control*, (56), pp. 1191-1197, 2011

[18] Thunberg J, Robinson J. Block backstepping, NDI and related cascade designs for efficient development of nonlinear flight control laws. *AIAA Guidance, Navigation and Control Conference and Exhibit*, 2008.

[19] Robinson J, Nilsson U. Design of a nonlinear autopilot for velocity and attitude control using block backstepping. *AIAA Guidance, Navigation and Control Conference and Exhibit*, 2005.

[20] Zhang Y H, Jiang J G. A novel disturbances compensating dynamic positioning of dredgers based on adaptive dynamic surface control. *WSEAS Transactions on Systems and Control*, (5), pp.323-332, 2010.

[21] Farrell J A, Polycarpou M, Sharma M, et al. Command filtered backstepping. *IEEE Transactions on Automatic Control*, (54), pp.1391-1395, 2009.

[22] Wang J H, Zhang J L, Yan J. A new second order nonlinear tracking differentiator and application. *International Conference On Computer Design And Applications*, pp. 318-322, 2010.